

9-3-2013

# Remnants of Spherical Shell Structures in Deformed Nuclei: The Impact of an $N = 64$ Neutron Subshell Closure on the Structure of $N \approx 90$ Gadolinium Nuclei

T. J. Ross

R. O. Hughes

C. W. Beausang

*University of Richmond*, cbeausan@richmond.edu

J. M. Allmond

C. Angell

*See next page for additional authors*Follow this and additional works at: <http://scholarship.richmond.edu/physics-faculty-publications>Part of the [Nuclear Commons](#)

## Recommended Citation

Ross, T. J., R. O. Hughes, C. W. Beausang, J. M. Allmond, C. T. Angell, M. S. Basunia, D. L. Bleuel, J. T. Burke, R. J. Casperson, J. E. Escher, P. Fallon, R. Hatarik, J. Munson, S. Paschalis, M. Petri, L. W. Phair, J. J. Ressler, and N. D. Scielzo. "Remnants of Spherical Shell Structures in Deformed Nuclei: The Impact of an  $N = 64$  Neutron Subshell Closure on the Structure of  $N \approx 90$  Gadolinium Nuclei." *Physical Review C* 88, no. 3 (September 3, 2013): 031301: 1-31301: 4. doi:10.1103/PhysRevC.88.031301.

---

**Authors**

T. J. Ross, R. O. Hughes, C. W. Beausang, J. M. Allmond, C. Angell, M. S. Basunia, D. L. Bleuel, J. T. Burke, R. J. Casperson, J. Escher, P. Fallon, R. Hatarik, J. Munson, S. Paschalis, M. Petri, L. Phair, J. J. Ressler, and N. D. Scielzo

## Remnants of spherical shell structures in deformed nuclei: The impact of an $N = 64$ neutron subshell closure on the structure of $N \approx 90$ gadolinium nuclei

T. J. Ross,<sup>1,2,\*</sup> R. O. Hughes,<sup>1</sup> C. W. Beausang,<sup>1</sup> J. M. Allmond,<sup>3</sup> C. T. Angell,<sup>4,†</sup> M. S. Basunia,<sup>5</sup> D. L. Bleuel,<sup>6</sup> J. T. Burke,<sup>6</sup> R. J. Casperson,<sup>6</sup> J. E. Escher,<sup>6</sup> P. Fallon,<sup>5</sup> R. Hatarik,<sup>5</sup> J. Munson,<sup>4</sup> S. Paschalis,<sup>5,‡</sup> M. Petri,<sup>5,‡</sup> L. W. Phair,<sup>5</sup> J. J. Ressler,<sup>6</sup> and N. D. Scielzo<sup>6</sup>

<sup>1</sup>Department of Physics, University of Richmond, Richmond, Virginia 23173, USA

<sup>2</sup>Department of Physics, University of Surrey, Guildford, Surrey, GU2 7JL, United Kingdom

<sup>3</sup>JHIR, Oak Ridge National Laboratory, Oak Ridge, Tennessee 37831, USA

<sup>4</sup>Department of Nuclear Engineering, University of California, Berkeley, California 94720, USA

<sup>5</sup>Nuclear Science Division, Lawrence Berkeley National Laboratory, Berkeley, California 94720, USA

<sup>6</sup>Lawrence Livermore National Laboratory, Livermore, California 94551, USA

(Received 4 April 2013; published 3 September 2013)

Odd-mass gadolinium isotopes around  $N = 90$  were populated by the  $(p,d)$  reaction, utilizing 25-MeV protons, resulting in population of low-spin quasineutron states at energies near and below the Fermi surface. Systematics of the single quasineutron levels populated are presented. A large excitation energy gap is observed between levels originating from the  $2d_{3/2}$ ,  $1h_{11/2}$ , and  $3s_{1/2}$  spherical parents (above the  $N = 64$  gap), and the  $2d_{5/2}$  (below the gap), indicating that the spherical shell model level spacing is maintained at least to moderate deformations.

DOI: 10.1103/PhysRevC.88.031301

PACS number(s): 25.40.Hs, 21.60.Cs, 21.10.Pc, 27.70.+q

From discrete energy levels in the hydrogen atom to band gaps in macroscopic solid-state systems to magic numbers in mesoscopic systems, such as metallic clusters and atomic nuclei, the clustering of energy levels in bound quantized systems is a widely occurring phenomenon. Systems with closed shells of particles tend to be symmetric and more stable than neighboring systems with a few more or less particles. It is well known that nuclei with magic numbers of protons and/or neutrons (2, 8, 20, 28, 82, 126) are spherically shaped and are more tightly bound than their neighboring “near-magic” isotopes. How these spherical and other deformed shell gaps change as a function of excitation energy, rotational frequency, or isospin is of continuing great interest. For example, the prediction and observation of deformed shell gaps in atomic nuclei led to the explosive interest in high-spin superdeformed states in the 1980s and 1990s [1,2]. For nuclei near the neutron drip line, changes from the familiar spherical magic numbers near stability are predicted [3].

Spectroscopy of such nuclei is typically complicated by the short-lived nature of such isotopes. For example, single-particle states in the region around doubly magic tin isotopes,  $^{100}\text{Sn}$  ( $N = 50$ ) and  $^{132}\text{Sn}$  ( $N = 82$ ), are extremely difficult to study directly. Indeed, most of the current information concerning  $^{131}\text{Sn}$  (i.e., single-particle states in the  $N = 50$ –82 shell) is taken from  $\beta$ -decay studies of  $^{131}\text{In}$  [4,5]. It has only recently become possible to perform direct reaction studies in the radioactive  $^{132}\text{Sn}$  region [6–9]. To date such studies have been used to populate the single-neutron particle states

in the region while results concerning the single-neutron *hole* structure have not been reported.

In this work, we employ the  $(p,d)$  one-neutron pickup reaction (in normal kinematics) to selectively populate quasineutron states in deformed gadolinium nuclei,  $A \sim 150$ . We use particle- $\gamma$  coincidence spectroscopy to identify the location (energy) and character (spin and parity) of the levels. The location of these single quasineutron structures qualitatively reflects the single-particle spherical shell structures observed in the  $N = 50$ –82 shell, almost 30 neutrons away ( $N \sim 64$ ). In this Rapid Communication we demonstrate the influence of an  $N = 64$  neutron subshell closure on the structure of these  $N \sim 90$  Gd nuclei.

The location of the spherical shell closures and their impact on the  $Z = 64$ ,  $N \sim 90$  region is, on first impression, relatively well understood, with major shells occurring for both protons and neutrons at  $N = Z = 50$  and  $N = Z = 82$ ; see Fig. 1. A proton subshell closure at  $Z = 64$  was first postulated in 1978 and inferred from a sharp increase in the  $2_1^+$  excitation energy in  $^{146}\text{Gd}_{82}$  [11]. Since then, the  $Z = 64$  subshell closure has become widely accepted in the field [12,13]. The existence of an  $N = 64$  neutron subshell closure has not been established despite much discussion of the issue [14–18].

The evolution of the single quasineutron levels, in the region of interest, as a function of deformation is shown in Fig. 1. While this diagram reflects a relatively simple calculation, the general trends serve as a valuable tool in interpreting the nuclear structure. The gadolinium isotopes of interest ( $^{153}\text{Gd}$ ,  $^{155}\text{Gd}$ , and  $^{157}\text{Gd}$ ) lie at the center of a region of rapid shape change from spherical ( $N \leq 90$ ) to deformed ( $N \geq 90$ ) character, with an observed deformation,  $\epsilon_2$ , ranging from  $\sim 0.21$ –0.34. The ground state of all three nuclei has spin parity of  $\frac{3}{2}^-$  [19–21] and is assigned as the  $\frac{3}{2}^-$  [521] Nilsson candidate (signified by the star in Fig. 1), which owes its origin to the  $f_{7/2}$  spherical orbital.

\*Current address: Department of Chemistry, University of Kentucky, Lexington, Kentucky 40506, USA.

†Current address: QBSD, JAEA, Tokai, Ibaraki 319-1195, Japan.

‡Current address: IKP, TU Darmstadt, 64289, Germany.

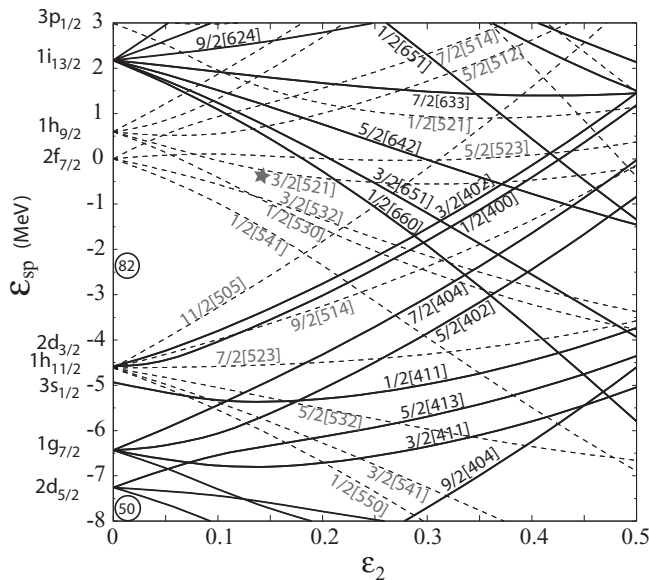


FIG. 1. The Nilsson diagram for neutrons in the region  $50 \lesssim N \lesssim 100$ . Shown are calculated single-neutron orbitals as a function of deformation ( $\epsilon_2$ ). The labels refer to the asymptotic Nilsson quantum numbers  $\Omega^\pi [N, n_z, \Lambda]$ . This labeling is ideally realized for large  $\epsilon_2$  deformations. While equal  $\Omega^\pi$  crossings at low deformations can obscure the orbital parentage, note that  $n_z + \Lambda = \ell_{\text{parent}}$ . Positive (negative) parity orbitals are denoted by solid (dashed) lines. This figure is taken from Ref. [10].

The  $(p,d)$  reaction serves as a precision tool which preferentially populates quasineutron hole states both near and far below the Fermi surface ( $\frac{3}{2}^- [521]$ ), including states based on the positive parity  $\frac{1}{2}^+ [400] - \frac{3}{2}^+ [402]$ , and  $\frac{5}{2}^+ [402] - \frac{7}{2}^+ [404]$  pseudo-spin-doublet pairs. The spacing between these orbital pairs is expected to remain approximately constant with increasing deformation and reflects the influence of a neutron subshell closure at  $N = 64$ . Levels based on the  $\frac{1}{2}^+ [400]$ ,  $\frac{3}{2}^+ [402]$ , and  $\frac{5}{2}^+ [402]$  orbitals are respectively the three most intensely populated positive-parity states, as is expected [10]. Candidates for the  $\frac{5}{2}^+ [402]$  orbital have been identified in  $^{153}\text{Gd}$ ,  $^{155}\text{Gd}$ , and  $^{157}\text{Gd}$  in the present  $(p,d)$  study and are discussed below.

While this  $N = 90$  region has long been a testing ground for various nuclear models, it is notable that the experiments upon which the majority of the low-lying level structure is based were carried out in the late 1960s and 1970s, typically using light-ion transfer reactions without  $\gamma$ -ray detection [19–21]. In 2010 a study of  $^{155}\text{Gd}$  by Allmond *et al.* [10] found several discrepancies in the single-neutron quasiparticle assignments. Most notably, a previous candidate for the  $\frac{7}{2}^+ [404]$  Nilsson state was reassigned as  $\frac{5}{2}^+ [402]$ , calling into question other  $\Delta\ell = 4\hbar$  assignments in the region; see also Ref. [22]. Building upon the results in  $^{155}\text{Gd}$ , and using particle- $\gamma$  coincidence analysis methods similar to those described in Ref. [10], we expand our study to odd-mass nuclei on either side of the  $N = 90$  region, namely to  $^{153}\text{Gd}$  and  $^{157}\text{Gd}$ .

The experiments were carried out at the 88-Inch Cyclotron at Lawrence Berkeley National Laboratory. In both cases,

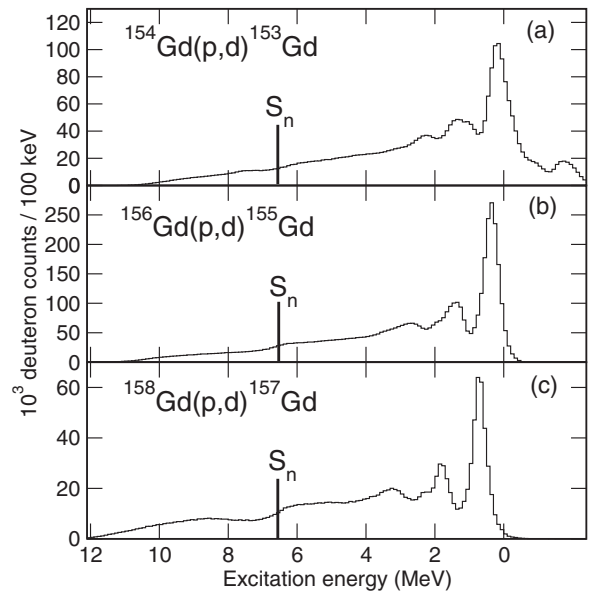


FIG. 2. Deuteron energy projections for the three reactions, plotted as a function of excitation energy in the residual nucleus: (a)  $^{154}\text{Gd}(p,d)\text{-}\gamma\text{-}^{153}\text{Gd}$  [counts below 0 keV correspond to the  $(p,d)$  reaction on target contaminants], (b)  $^{156}\text{Gd}(p,d)\text{-}\gamma\text{-}^{155}\text{Gd}$  [10], and (c)  $^{158}\text{Gd}(p,d)\text{-}\gamma\text{-}^{157}\text{Gd}$ .

a 25-MeV ( $\sim 2.5$ -enA) proton beam was used to study the  $(p,d-\gamma)$  reaction on even-even  $^{154,156,158}\text{Gd}$  targets. Outgoing charged particles were detected using the Silicon Telescope Array for Reaction Studies (STARS) [23], which consisted of a segmented  $\Delta E$ - $E$  telescope, allowing for measurement of the energy and angle of the emitted deuteron. Coincident  $\gamma$  rays were detected using an array of five Compton-suppressed clover Ge detectors, the Livermore Berkeley Array for Collaborative Experiments (LIBERACE) [23]. Events were recorded when at least one  $\gamma$  ray and one charged particle were measured in coincidence. Further details about the experimental setup can be found in Refs. [10,24,25].

The deuteron spectrum, plotted as a function of excitation energy for each of these three reactions, is shown in Fig. 2. The three spectra exhibit very similar properties. At low excitation energies, below  $\sim 700$  keV, there is a large peak which corresponds to direct population of a cluster of low-lying states. A second peak is observed in each of the spectra at higher excitation energies, centered closer to 1.5 MeV. This peak corresponds to a second cluster of directly populated states. While the resolution of the silicon detectors is insufficient to resolve the individual levels in these clusters, they can be isolated by a coincidence requirement with a discrete  $\gamma$  ray. A brief example utilizing a previously unobserved 940.7-keV  $\gamma$  ray in  $^{153}\text{Gd}$  is discussed. The solid spectrum in Fig. 3(a) shows the deuterons detected in coincidence with the 941-keV transition. The observed peak corresponds to the direct population by the  $(p,d)$  reaction of a level at  $1181 \pm 20$  keV, which subsequently decays via the 941-keV  $\gamma$ -ray transition. A reverse-coincidence requirement (placed upon this deuteron energy) returns all  $\gamma$  rays in coincidence with the selected excitation energy region, Fig. 3(b). As expected, the 941-keV  $\gamma$  ray is prominent, as are several other  $\gamma$  rays, which now also

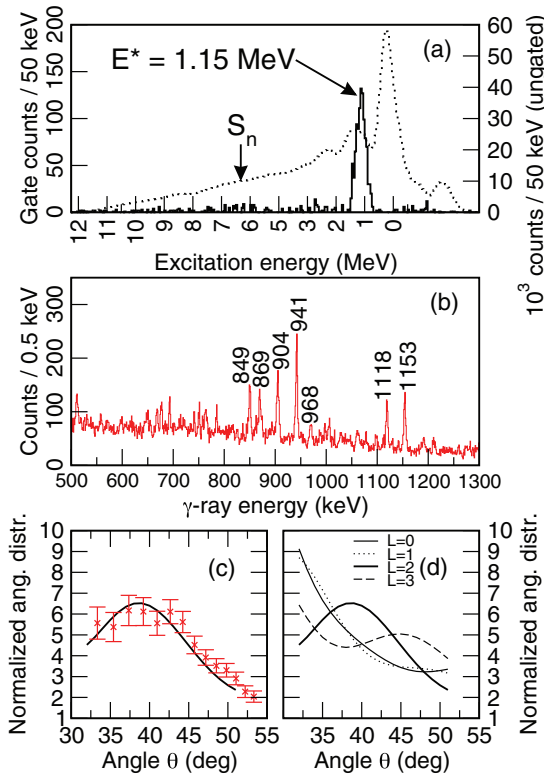


FIG. 3. (Color online) (a) Solid spectrum: Deuterons measured in coincidence with the newly observed 940.7-keV  $\gamma$  ray in  $^{153}\text{Gd}$ . Dashed spectrum: The total deuteron spectrum showing *all* population of  $^{153}\text{Gd}$ . (b)  $\gamma$  rays detected in coincidence with deuterons of energy  $1181 \pm 20$  keV. (c) The angular distribution of deuterons which populate the 1153-keV level. (d) Calculated DWBA curves for angular momentum transfers  $\Delta\ell = 0, 1, 2$ , and  $3\hbar$ .

become candidates for transitions depopulating the 1181-keV level. Combining these measurements of initial excitation energy and  $\gamma$ -ray decay, with our knowledge of the low-lying level scheme, the newly observed coincident  $\gamma$  rays typically fit into the level scheme in one unique arrangement, allowing a very accurate measurement of the new level energy,  $1152.9 \pm 1$  keV. In addition, the angular distribution of the deuterons which populate the level has a distinct shape, which allows us to deduce the angular momentum transferred and thus a measure of the spin and parity of this state. In this case the observed angular distribution is best fit by a distorted wave Born approximation (DWBA) calculation corresponding to  $\Delta\ell = 2\hbar$  transfer, Figs. 3(c) and 3(d). Further details concerning the DWBA calculations can be found in Refs. [10,26]. Based upon this angular-momentum transfer and the observed  $\gamma$ -ray decays the level is assigned spin parity  $\frac{5}{2}^+$ . The level is assigned as the  $\frac{5}{2}^+$  [402] Nilsson candidate on the basis of its high relative population cross-section (the level has the highest  $2\hbar$  transfer cross section and is the third most intensely populated positive-parity state) and the observed  $\gamma$ -ray decay pattern.

Similarly in  $^{155}\text{Gd}$ , a  $\frac{5}{2}^+$  level at 1296 keV was assigned as the  $\frac{5}{2}^+$  [402] Nilsson candidate, Ref. [10]. In  $^{157}\text{Gd}$  the situation is slightly different and four discrete levels, above 1500-keV excitation energy, are populated by  $\Delta\ell = 2\hbar$  transfer. Based

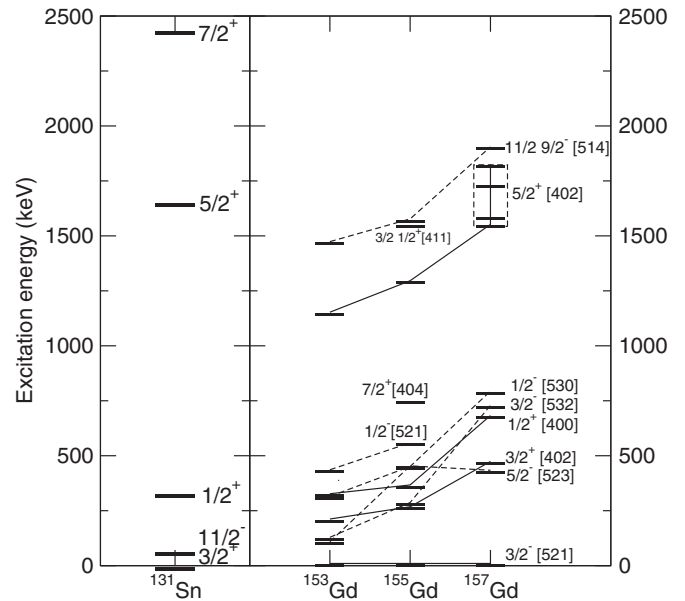


FIG. 4. Right: Excitation energy of the levels observed in  $^{153}\text{Gd}$ ,  $^{155}\text{Gd}$  [10], and  $^{157}\text{Gd}$ . Levels are labeled by their assigned Nilsson structures. Positive- (negative-) parity states are denoted by solid (dashed) lines. Left: Excitation of the known single-particle states in  $^{131}\text{Sn}$ , [4,5].

upon the relative cross-sections and  $\gamma$ -ray decays, levels at 1589 and 1825 keV are potential candidates and therefore a firm assignment is not made. Further details of these and other assignments can be found in Refs. [10,27].

Partial level schemes for the three isotopes are shown in Fig. 4 (right panel). All levels shown are directly populated in this work by the  $(p,d)$  reaction. Levels below  $\sim 700$  keV were previously observed and are confirmed in this work. Levels above  $\sim 700$  keV are observed and/or assigned and all have newly associated  $\gamma$ -ray decays. For more details, see Ref. [27]. For clarity only the lowest energy level of each Nilsson candidate directly populated by the  $(p,d)$  reaction is shown.

As mentioned previously these nuclei straddle a region of *rapid* shape change from vibrational ( $^{153}\text{Gd}$ ) to transitional ( $^{155}\text{Gd}$ ) to rotational ( $^{157}\text{Gd}$ ) character. This evolution is reflected in the changing excitation energy of the levels in these nuclei. However, the most striking feature in these level schemes is the large gap,  $\sim 0.5$  MeV, between levels below  $\sim 700$  keV and greater than  $\sim 1200$  keV. This excitation energy gap corresponds to the trough between the two peaks in the deuteron spectra, Fig. 2. Indeed, studies of neighboring rare-earth nuclei have also yielded light-ion spectra which exhibit a similar feature [22,28]. Upon inspection of the Nilsson diagram, Fig. 1, it becomes apparent that the low-lying levels can be associated with states built on orbitals lying relatively near to the neutron Fermi surface. The levels at higher excitation energies can be associated with deeper lying states, lying below the deformed shell gap indicated in Fig. 1. These states and this deformed shell gap in turn originate from the  $N = 64$  spherical subshell closure, almost 30 neutrons away from the Fermi surface of these  $N \sim 90$  nuclei.

The location of the band heads of the pseudospin partner pairs,  $\frac{3}{2}^+$  [402]– $\frac{1}{2}^+$  [400] and  $\frac{7}{2}^+$  [404]– $\frac{5}{2}^+$  [402], is particularly

revealing [29,30]. The relative energy spacing of these four upsloping and parallel orbitals in these three Gd isotopes remains approximately constant in spite of the effects of deformation and reflects the spacing of the spherical parents that they originate from. These spherical orbitals ( $2d_{3/2}$ ,  $3s_{1/2}$ ,  $1g_{7/2}$ , and  $2d_{5/2}$ ) play a major role in the single-neutron structure of nuclei lying near the exotic neutron-rich doubly magic  $^{132}\text{Sn}$  nucleus. For example,  $^{131}\text{Sn}$  is just one neutron away from doubly magic  $^{132}\text{Sn}$  and its single-neutron hole energies closely reflect the spherical shell structure. The single-particle structure of  $^{131}\text{Sn}$ , as established by  $\beta$ -decay studies [4,5], is also shown in Fig. 4 (left panel). There is a large gap in the  $^{131}\text{Sn}$  level scheme which is qualitatively reflected by the spacing of the positive-parity Nilsson orbitals in the gadolinium isotopes.

While a state built on the  $\frac{7}{2}^+$ [404] orbital has been proposed in  $^{155}\text{Gd}$ , candidate states are not identified in either  $^{153}\text{Gd}$  or  $^{157}\text{Gd}$ . In  $^{155}\text{Gd}$  the  $\frac{7}{2}^+$ [404] candidate state is observed at 752 keV, placing it at the top of the cluster of low-lying states in Fig. 2. Indeed firm assignments of the  $\frac{7}{2}^+$ [404] Nilsson orbital have proved troublesome throughout this deformed region. The only other adopted assignment is found in  $^{161}\text{Dy}$ , where the level was assigned based upon an observed  $4\hbar$  angular-momentum transfer following the  $(d,t)$  reaction. Experimental efforts to populate this state in these nuclei using, for example, the  $(d,t)$  or  $(^3\text{He},\alpha)$  reaction (both expected to populate higher spin states than the current proton induced reaction) would be valuable.

The location of the negative-parity orbitals in the region is also revealing. The upsloping  $\frac{11}{2}^-$ [505] orbital, originating from  $1h_{11/2}$ , is expected to remain somewhat parallel to the positive-parity orbitals mentioned above; see Fig. 1. Indeed, in the literature [19–21], states built upon this orbital are firmly established at low excitation energies for each of the three isotopes, in agreement with the structure of  $^{131}\text{Sn}$ , Fig. 4. This state is not directly populated by the  $(p,d)$  reaction in this work. In contrast, candidates for the  $\frac{11}{2}^-$  member of the

$\frac{9}{2}^-$ [514] orbital are directly populated in this work but at very high excitation energies, above the gap. Our calculations place this orbital much lower in energy, in the gap between the two clusters of levels, possibly indicating that the location of the spherical  $1h_{11/2}$  orbital is somewhat too high in Fig. 1.

In conclusion, a large ( $\sim 500$ – $700$  keV) energy gap is revealed at high excitation energies in the spectrum of quasineutron hole states in  $A \sim 150$  gadolinium isotopes populated by the  $(p,d)$  reaction. It is striking that such a strong effect is reflected when studying the structure of the nucleus so far below the Fermi surface. The selectivity of the  $(p,d)$  reaction mechanism allows the isolation of this deformed shell gap from the complexity of the full level scheme where a plethora of excitations including neutron-particle and neutron-hole states, proton excitations, collective excitations, etc., can be observed. This gap in the sub-Fermi surface level scheme owes its origin to a spherical neutron subshell closure at  $N = 64$ , which plays a major role in the structure of nuclei in the region around  $^{132}\text{Sn}$ , and demonstrates the persistence of this structure in these deformed nuclei with almost 30 more neutrons. While reactions such as  $(d,p)$ ,  $(^{13}\text{C},^{12}\text{C})$ , and  $(^9\text{Be},^8\text{Be})$  in inverse kinematics can and have been used to populate single-neutron states *above* the Fermi surface, no such work has yet been reported on the nearby neutron hole states (discussed here) lying just *below* the  $^{132}\text{Sn}$  Fermi surface.

The authors thank the 88-Inch Cyclotron operations and facilities staff for their help in performing this experiment. This work was performed under the auspices of the National Science Foundation and the US Department of Energy by the University of Richmond under Grants No. DE-FG52-06NA26206 and No. DE-FG02-05ER41379, Lawrence Livermore National Laboratory under Contracts No. W-7405-Eng-48 and No. DE-AC52-07NA27344, and Lawrence Berkeley National Laboratory under Contract No. DE-AC02-05CH11231 with partial support through the TORUS topical collaboration.

- 
- [1] R. V. F. Janssens and T. L. Khoo, *Annu. Rev. Nucl. Part. Sci.* **41**, 321 (1991).  
 [2] P. J. Twin *et al.*, *Phys. Rev. Lett.* **57**, 811 (1986).  
 [3] T. Otsuka *et al.*, *Phys. Rev. Lett.* **87**, 082502 (2001).  
 [4] Yu. Khazov, I. Mitropolsky, and A. Rodionov, *Nucl. Data Sheets* **107**, 2715 (2006).  
 [5] B. Fogelberg *et al.*, *Phys. Rev. C* **70**, 034312 (2004).  
 [6] K. J. Jones *et al.*, *Nature (London)* **465**, 454 (2010).  
 [7] K. J. Jones *et al.*, *Phys. Rev. C* **84**, 034601 (2011).  
 [8] R. L. Kozub *et al.*, *Phys. Rev. Lett.* **109**, 172501 (2012).  
 [9] J. M. Allmond *et al.*, *Phys. Rev. C* **86**, 031307(R) (2012).  
 [10] J. M. Allmond *et al.*, *Phys. Rev. C* **81**, 064316 (2010).  
 [11] M. Ogawa, R. Broda, K. Zell, P. J. Daly, and P. Kleinheinz, *Phys. Rev. Lett.* **41**, 5 (1978).  
 [12] R. R. Chasman, *Phys. Rev. C* **21**, 456 (1980).  
 [13] P. Mukherjee, R. Bhattacharya, and I. Mukherjee, *Phys. Rev. C* **24**, 1810 (1981).  
 [14] T. Sumikama *et al.*, *Phys. Rev. Lett.* **106**, 202501 (2011).  
 [15] H. Hua *et al.*, *Phys. Rev. C* **69**, 014317 (2004).  
 [16] C. Piller *et al.*, *Phys. Rev. C* **42**, 182 (1990).  
 [17] V. R. Green *et al.*, *Phys. Lett. B* **173**, 115 (1986).  
 [18] R. Wenz *et al.*, *Z. Phys. A* **303**, 87 (1981).  
 [19] R. G. Helmer, *Nucl. Data Sheets* **107**, 507 (2006).  
 [20] C. W. Reich, *Nucl. Data Sheets* **104**, 1 (2005).  
 [21] R. G. Helmer, *Nucl. Data Sheets* **103**, 565 (2004).  
 [22] N. Blasi *et al.*, *Nucl. Phys. A* **624**, 433 (1997).  
 [23] S. R. Leshner *et al.*, *Nucl. Instrum. Methods A* **621**, 286 (2010).  
 [24] T. J. Ross *et al.*, *Phys. Rev. C* **85**, 051304(R) (2012).  
 [25] T. J. Ross *et al.*, *Phys. Rev. C* **86**, 067301 (2012).  
 [26] P. D. Kunz, DWUCK4, University of Colorado (unpublished).  
 [27] T. J. Ross *et al.* (unpublished).  
 [28] S. Gales, G. M. Crawley, D. Weber, and B. Zwieglinski, *Nucl. Phys. A* **398**, 19 (1983).  
 [29] K. T. Hecht and A. Adler, *Nucl. Phys. A* **137**, 129 (1969).  
 [30] A. Arima *et al.*, *Phys. Lett. B* **30**, 517 (1969).